Skarjune, R., & Oldfield, E. (1979) *Biochemistry 18*, 5903.
Solomon, I. (1958) *Phys. Rev. 110*, 61.
Spiess, H. W., & Sillescu, H. (1981) *J. Magn. Reson. 42*, 381.
Stamatoff, J., Feuer, B., Guggenheim, H., Tellez, G., & Yamane, T. (1982) *Biophys. J. 38*, 217.
Sundaralingam, M. (1972) *Ann. N.Y. Acad. Sci. 195*, 324.
Vaughan, D. J., & Keough, K. M. (1974) *FEBS Lett. 47*, 158.
Weissbach, H., & Sprinson, D. B. (1953) *J. Biol. Chem. 203*, 1031.
Wilkinson, D. A., & Nagle, J. F. (1981) *Biochemistry 20*, 187.
Wittebort, R. G., Schmidt, C. F., & Griffin, R. G. (1981) *Biochemistry 20*, 4223.
Wittebort, R. G., Blume, A., Huang, T-H., Das Gupta, S. K., & Griffin, R. G. (1982) *Biochemistry 21*, 3487.

Carbon-13 and Deuterium Nuclear Magnetic Resonance Study of the Interaction of Cholesterol with Phosphatidylethanolamine†

A. Blume‡ and R. G. Griffin*

ABSTRACT: Mixtures of dipalmitoylphosphatidylethanolamine (DPPE) and cholesterol (CHOL) have been studied with solid-state ^{13}C and ^{2}H nuclear magnetic resonance (NMR) techniques. DPPE was ^{13}C labeled at the carbonyl group of the *sn*-2 chain, and ^{2}H was introduced at the 4 position of the *sn*-2 chain and the 1 position of the ethanolamine head group. The ^{13}C and ^{2}H spectra of each labeled lipid were studied as a function of temperature and CHOL concentration, and the results indicate three distinguishable temperature–composition regions. In region I, which occurs at low temperatures and CHOL concentrations, the ^{13}C and ^{2}H spectra are similar to those observed for pure DPPE in its gel phase. In region II, which occurs at higher temperatures or CHOL concentrations, the *sn*-2 $^{13}C{=}O$ spectra of DPPE/CHOL mixtures display two components, indicating the coexistence of two conformationally and dynamically inequivalent DPPE molecules. One of these is similar to gel-state DPPE, while the second "fluid" fraction displays some liquid-crystalline character. The two-component ^{13}C spectra can be simulated quantitatively with a two-parameter chemical exchange model that permits the fraction of each form and the exchange rate to be determined as a function of temperature and composition. The ^{2}H spectra observed in region II do not exhibit two components in an obvious way. Nevertheless, with some reasonable assumptions, the ^{2}H spectra obtained from chain-labeled DPPE can also be simulated with a two-component model with the exchange rates and fractional populations obtained from the ^{13}C results. The calculations predict not only the line shapes but also the losses in spectral intensity arising from use of the quadrupole echo technique. Furthermore, the ^{2}H spectra show that with increasing temperature the fluid fraction observed in region II undergoes a transition to a higher degree of disorder, and should therefore not be labeled "liquid crystalline". In region III, which occurs at high temperatures and CHOL concentrations, both the ^{13}C and ^{2}H spectra are those expected of liquid-crystalline lipid. The NMR results are compared to, and found to be different from, those obtained with calorimetric investigations. It is suggested that these differences are due to the small domains present in DPPE/CHOL mixtures that lead to phase transitions of low cooperativity. Some metastability of the DPPE/CHOL system was observed at high CHOL concentrations and low temperatures.

Cholesterol (CHOL)[1] occurs in many biological membranes at relatively high levels, and as a consequence the properties of phospholipid/CHOL mixtures have been extensively investigated [for a review, see Demel & deKruijff (1976)]. Generally, the addition of CHOL to PC bilayers leads to a broadening of the gel to liquid-crystalline phase transition and to a decrease of the calorimetrically observed transition enthalpy (Ladbrooke et al., 1968). Recently, high-sensitivity DSC experiments have indicated that this transition is observable at CHOL concentrations up to about 50 mol % (Mabrey et al., 1978; Estep et al., 1978). Moreover, monolayer experiments have shown that addition of CHOL to liquid crystalline phase lipids can result in a condensation of the lipid lattice (Shah & Schulman, 1967; Phillips, 1972, Müller-Landau & Cadenhead, 1979). Thus, a simple and commonly used interpretation of the DSC and monolayer experiments is that CHOL orders the liquid-crystalline phase and disorders the gel phase of phospholipid bilayers. Nevertheless, a number of other more subtle effects have been observed in lipid/CHOL mixtures, and as a result there have been numerous investigations devoted to understanding the detailed features of PC/CHOL phase diagrams (Shimshick & McConnell, 1973; Estep et al., 1978; Mabrey et al., 1978; Gershfeld 1978; Pink & Chapman, 1979; Rubinstein et al., 1979, 1980; Lentz et al., 1980; Copeland & McConnell, 1980; Cornell et al., 1979; Owicki & McConnell, 1980; Melchior et al., 1980; Snyder & Friere, 1980; Recktenwald & McConnell, 1981).

Because most studies have focused on PC/CHOL mixtures, there is a paucity of information available on other phospholipid/CHOL systems. For example, it is only in the recent

† From the Francis Bitter National Magnet Laboratory, Massachusetts Institute of Technology, Cambridge, Massachusetts 02139. *Received April 20, 1982.* This research was supported by the National Institutes of Health (GM 23289, GM 25505, and RR00995) and by the National Science Foundation through its support of the Francis Bitter National Magnet Laboratory (C-670). A.B. was supported by a research scholarship from the Deutsche Forschungsgemeinschaft (BL 182/2 4).

‡ Present address: Institut für physikalische Chemie II, D-7800 Freiburg, Federal Republic of Germany.

[1] Abbreviations: CHOL, cholesterol; DPPC, dipalmitoylphosphatidylcholine; DPPE, dipalmitoylphosphatidylethanolamine; NMR, nuclear magnetic resonance; ESR, electron spin resonance; DSC, differential scanning calorimetry; TLC, thin-layer chromatography.

0006-2960/82/0421-6230$01.25/0

past that sphingomyelin and PE/CHOL mixtures have been investigated with DSC and X-ray experiments (Estep et al., 1979; Calhoun & Shipley, 1979; Blume, 1980). As a consequence relatively little is known about the microscopic properties of these systems, and for this and other reasons we have begun an investigation of such lipid/CHOL mixtures employing solid-state ^{13}C and ^{2}H NMR spectroscopy. In this report we discuss results for the DPPE/CHOL system.

There are a number of features of the DPPE/CHOL system that make it an attractive candidate for these studies. First, the thermal behavior of diacyl-PE's is relatively simple when compared to diacyl-PC's. In the gel phase PE's exist in an L_β lattice and transform directly to an L_α lattice at a well-defined main transition temperature, T_c. In contrast, diacyl-PC's undergo a pretransition, from an $L_{\beta'}$ to a $P_{\beta'}$ phase, a few degrees below the T_c, and we have recently shown that this pretransition results in changes in the molecular conformation and dynamic properties of some of the lipid molecules in the bilayer. Specifically, there is a conformational change in the glycerol backbone region, as well as a partial, although not dramatic, melting of the acyl chains (Wittebort et al., 1981, 1982; Blume et al., 1982a,b), and both of these effects are observable in the NMR spectra. Interestingly enough, CHOL induces quite similar changes, and for this reason it is difficult to dissect the effects of CHOL from those due to the presence of the $P_{\beta'}$ phase. Since PE's do not exhibit a $P_{\beta'}$ phase, any changes in their spectra must be induced by, and are therefore assignable to, the presence of CHOL. In addition, this system has been investigated with high-sensitivity calorimetry (Blume, 1980), so that the temperatures for the onset and completion of melting are fairly well established, and can be compared with the NMR results. Finally, DPPE has a relatively high T_c (64 °C), and as a result a wide temperature range below the main transition can be investigated without cooling below the freezing point of water.

In this work we have studied mixtures where DPPE was ^{13}C labeled at the *sn*-2 C=O group or ^{2}H labeled either at the 4 position of the *sn*-2 chain or at the 1 position of the ethanolamine head group. These labels were chosen to detect alterations in the glycerol backbone, acyl chains, and the head group regions, respectively. The NMR spectra provide detailed information on the changes in the molecular conformation and dynamic properties of DPPE molecules as a function of temperature and composition. At low temperatures and CHOL concentrations, we observe a region where DPPE exists in what appears to be a gel state. With either increasing temperature or mole percent CHOL, a fraction of these molecules transform to "fluid" lipids, and these coexist and exchange with gel-state lipids over a wide temperature–composition region. As will be seen below, this fluid fraction has some conformational and dynamic properties of L_α-phase DPPE. However, it differs markedly in at least one other respect and should therefore not be thought of as a liquid-crystalline fraction. This point is clearly illustrated by the fact that at sufficiently high temperatures and CHOL concentrations the fluid lipids undergo a cooperative transition to a higher degree of disorder—e.g., to a liquid-crystalline phase. Finally, a comparison of the NMR results with data from DSC studies shows that there is not always a direct correlation between the two experiments. The interpretation of the NMR data in terms of a thermodynamic phase diagram must therefore be done with caution.

Materials and Methods

2[1-^{13}C]DPPE, 2[4,4-$^{2}H_2$]DPPE, and $^{+}NH_3$–CH_2–CD_2–DPPE were synthesized as described previously (Blume et al., 1982a). ^{13}C and ^{2}H NMR spectra were obtained on a home-built solid-state pulse spectrometer operating at 73.9 MHz for ^{13}C and 45.1 MHz for ^{2}H. ^{13}C spectra were recorded with a Hahn spin-echo or cross-polarization with a 180° refocusing pulse (Pines et al., 1973; Griffin, 1981). The ^{13}C $\pi/2$ pulse width was ~ 3 μs. For minimization of radio frequency heating, low ^{1}H decoupling power as well as long recycle delays of 5 s was used. ^{2}H spectra were recorded with a quadrupole echo sequence (Davis et al., 1976) with a pulse spacing of 40 μs. The ^{2}H $\pi/2$ pulse width was 1.7–2.0 μs. Dwell times were 0.2 or 0.5 μs for gel-state species, and 2 μs for spectra in the liquid-crystalline state. Recycle delays were 0.2 s. Phase cycling was used to eliminate pulse transients, and spectra were detected in quadrature. The procedure employed in recording the absolute-intensity ^{2}H spectra shown in Figure 6 is described elsewhere (Blume et al., 1982a).

Samples consisted of 50–100 mg of lipid. DPPE and cholesterol were mixed in chloroform; the solvent was evaporated in a stream of nitrogen at 60 °C. The lipid mixtures were then dried under high vacuum for 24 h to remove residual solvent. The lipid mixtures were then dispersed in ^{2}H-depleted water ($\sim$70 wt % H_2O, Aldrich Chemicals, Milwaukee, WI), sealed in 7-mm glass tubes, and equilibrated at 70 °C for 1 h prior to taking spectra. Because of this rather high temperature, the samples were always checked for decomposition with TLC both before and after completion of the NMR experiments.

Results

In previous investigations we have shown that the *sn*-2 ^{13}C=O powder pattern of a phospholipid undergoes a dramatic narrowing at the gel to liquid-crystalline phase transition (Wittebort et al., 1981, 1982; Blume et al., 1982a,b). In the gel phase an axially symmetric spectrum of about 100-ppm width is observed, whereas in the L_α phase this pattern narrows to an isotropic-like line of about $\sim$1-ppm breadth. This same spectral behavior can be induced by addition of CHOL to the bilayer (Wittebort et al., 1982) and is illustrated in Figure 1 for the DPPE/CHOL system. In Figure 1a are shown temperature-dependent ^{13}C=O spectra for pure DPPE, and parts b–f of Figure 1 illustrate the result of the addition of 10, 20, 30, 40, and 50 mol % CHOL to the pure lipid. Note that as the CHOL concentration is increased, the narrow L_α-like spectrum appears at progressively lower temperatures. Furthermore, at temperatures slightly below those at which the single line is present, there invariably exists a temperature region over which two-component spectra are observed. Since the components of these spectra consist of an L_α-like line superimposed on an L_β-like powder pattern, they indicate the coexistence of two long-lived conformations of DPPE molecules. Moreover, when both components are present, the L_α line is noticeably broadened, suggesting the presence of chemical exchange between the two components of the spectrum. The computer simulations in the right column of parts b–f of Figure 1 were performed assuming such an exchange process, and inspection of the line shapes shows that the computer results reproduce the experimental spectra quite well. In performing these calculations, we have assumed two types of ^{13}C=O tensors, one oriented with its unique axis at the "magic angle" [$\theta = \cos^{-1}(1/3^{1/2})$], which produces the L_α-like line, and a second with $\theta \simeq 28°$, which results in the L_β powder pattern. Both tensors are constrained to execute rapid (on the ^{13}C time scale) jumps about the molecular long axis, and they are permitted to exchange. The details of this model, and various unacceptable alternatives to it, have been described elsewhere (Wittebort et al., 1981, 1982). The two parameters that are varied to reproduce the line shapes are the exchange

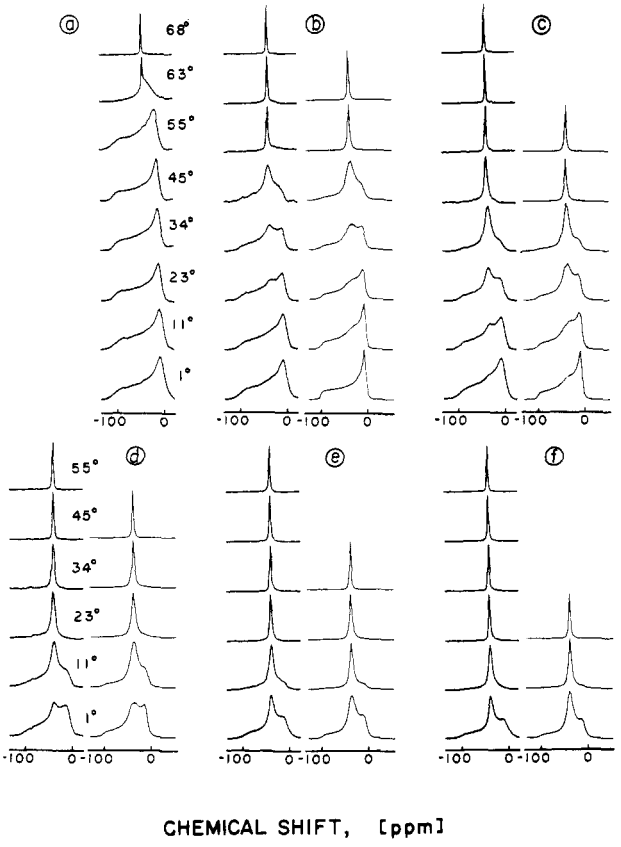

FIGURE 1: Proton-decoupled ^{13}C NMR spectra of 2[1-^{13}C]DPPE and 2[1-^{13}C]DPPE/cholesterol mixtures as a function of temperature (°C). On the right next to the experimental spectra are computer simulations from the line-shape simulation program described in the text. The parameters used in the simulations for the fractions of both components and for the exchange rates are shown in Figures 3 and 4. Only the $^{13}C{=}O$ resonance line is shown. Samples contained 50–80 wt % H_2O. (a) 0, (b) 10, (c) 20, (d) 30, (e) 40, and (f) 50 mol % CHOL, respectively.

rate and the fraction of (fluid) L_α-like lipid, f_F.

In Figure 2 we have plotted f_F obtained from these simulations in two ways. In Figure 2a we show this parameter as a function of temperature at constant CHOL concentration, whereas in Figure 2b we show the same data, but plotted as a function of CHOL concentration at constant temperature. Also included in Figure 2a are the normalized heat capacity curves from DSC studies of this system (Blume, 1980). Note that these curves are displaced to higher temperature when compared to the ^{13}C NMR results, a point that will be discussed below. In Figure 3a the exchange rates are plotted as a function of temperature at constant CHOL concentration, whereas in Figure 3b we again show the same data as a function of CHOL concentration, but at constant temperature.

In Figure 4 are illustrated ^2H spectra of 2[4,4-$^2H_2$]DPPE in pure form and in the presence of 10, 30, and 50 mol % CHOL. A cursory examination of these spectra shows that addition of CHOL to the bilayer results in the appearance of a sharp axially symmetric spectrum at progressively lower temperatures, and it is tempting to associate these sharp spectra with liquid-crystalline lipids. In Figure 5a we have plotted the residual quadrupole splittings $\Delta\nu_{Q\perp}$, obtained from the sharp axially symmetric component of these spectra, as function of CHOL concentration at constant temperature. Inspection of these plots shows that at some temperatures—e.g., $T \geq 63$ °C—the term L_α would be reasonable accurate since $\Delta\nu_{Q\perp}$ departs from the pure L_α phase value (~30 kHz) by ≤20%. However, for $T < 63$ °C the splittings are 1.5–2

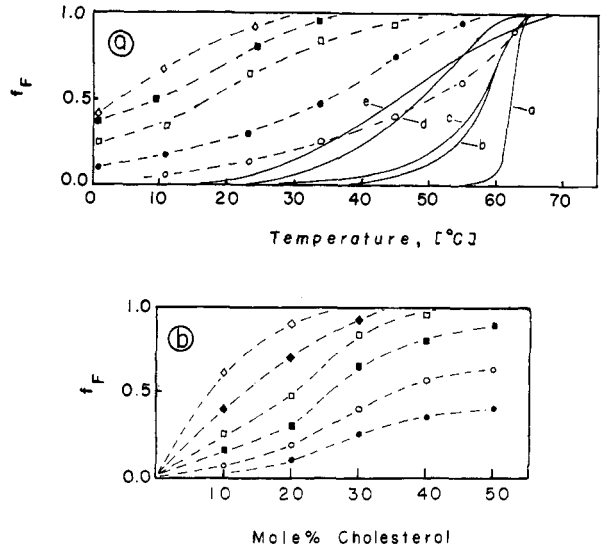

FIGURE 2: (a) Fraction of fluid lipid, f_F, obtained from line-shape simulations of the ^{13}C NMR spectra in Figure 1 vs. temperature: (○) 10, (●) 20, (□) 30, (■) 40, and (◇) 50 mol % CHOL, respectively. Solid lines (—) are transition curves obtained by numerical integration of the calorimetric curves from Blume (1980): (a) 0, (b) 10, (c) 20, (d) 30, and (e) 40 mol % CHOL. (b) f_L vs. CHOL content: (●) 1 °C, (○) 11 °C, (■) 23 °C, (□) 34 °C, (◆) 45 °C, and (◇) 55 °C.

times those observed for pure L_α-phase DPPE. This point is perhaps better illustrated in Figure 5b where these data are shown as a function of temperature at constant CHOL concentration. Clearly $\Delta\nu_{Q\perp}$ is ~50 kHz at temperatures below approximately 55 °C, and thus, even though these lipids are fluid, the label "L_α" is less appropriate.

In addition, there is another rather interesting feature of the ^2H chain spectra that should be mentioned. The *sn*-2 $^{13}C{=}O$ spectra in Figure 1 clearly show the presence of two components that we have tentatively associated with gel-like and fluid-like lipid molecules. The ^2H spectra shown in Figure 4 (and in Figure 8 below) are remarkable in that they conspicuously lack a second well-resolved component. Note, however, that in many cases the line shapes are broadened, and we believe this broadening is probably due to exchange between gel-like and fluid-like domains. In Figure 6 we show experimental spectra for 2[4,4-$^2H_2$]DPPE/20% CHOL together with computer simulations that illustrate the effects observed in ^2H spectra in this type of situation. Note that these spectra and the simulations are plotted on an absolute intensity scale, and at lower temperatures (<45 °C) the spectral intensity is depressed in part due to the exchange process. In Figure 7 we compare the calculated, integrated spectral intensities with those obtained experimentally for the 20% CHOL sample. In addition this figure includes similar experimental data for pure 2[4,4-$^2H_2$]DPPE and for 2[4,4-$^2H_2$]DPPE/40% CHOL. These figures will be discussed in more detail in the following section.

In Figure 8 are illustrated ^2H spectra of $^+NH_3$–CH_2–CD_2–DPPE in pure DPPE bilayers (Figure 8a) and in the presence of 10, 30, and 50 mol % CHOL (Figure 8b–d). At low temperatures these spectra are broad and featureless, but with either increasing temperature or CHOL content a sharp axially symmetric line shape appears. In Figure 9a we have plotted $\Delta\nu_{Q\perp}$ obtained from these spectra as a function of mole percent CHOL and it is seen that the results are somewhat different from those observed for the acyl chains. In particular there is only an approximately 10–20% change in this parameter, and it decreases with increasing CHOL content. In the acyl chain spectra the opposite behavior was sometimes

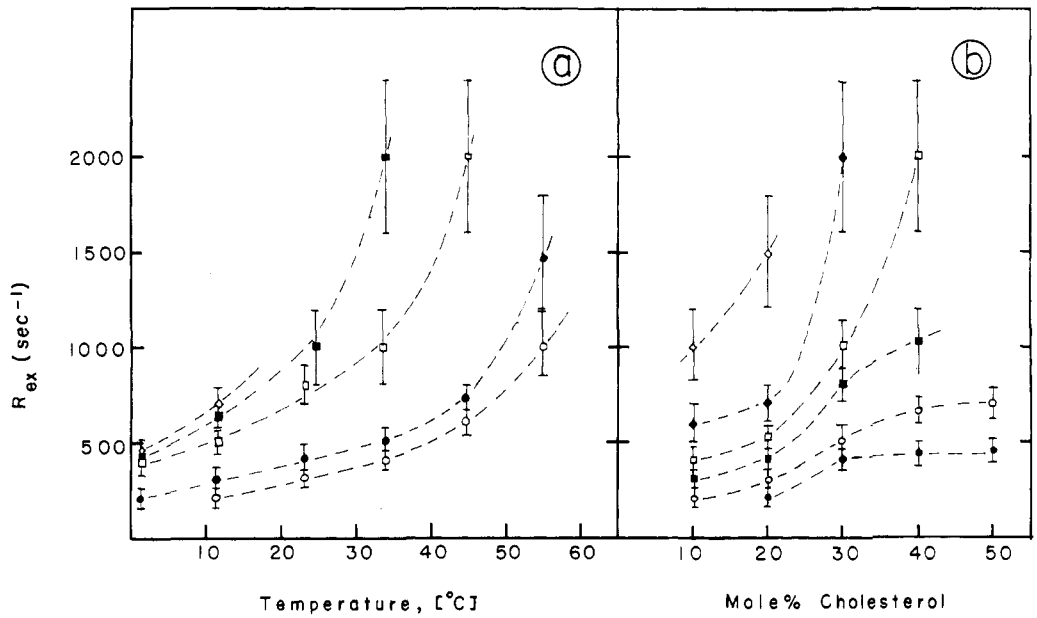

FIGURE 3: (a) Exchange rate constants, R_{ex} (s^{-1}), obtained from line-shape simulations vs. temperature. Error bars denote uncertainties in the values of R_{ex}. Note they become large when R_{ex} approaches the fast-exchange limit and f_F approaches unity. (b) R_{ex} vs. cholesterol content. For explanation of symbols see Figure 2.

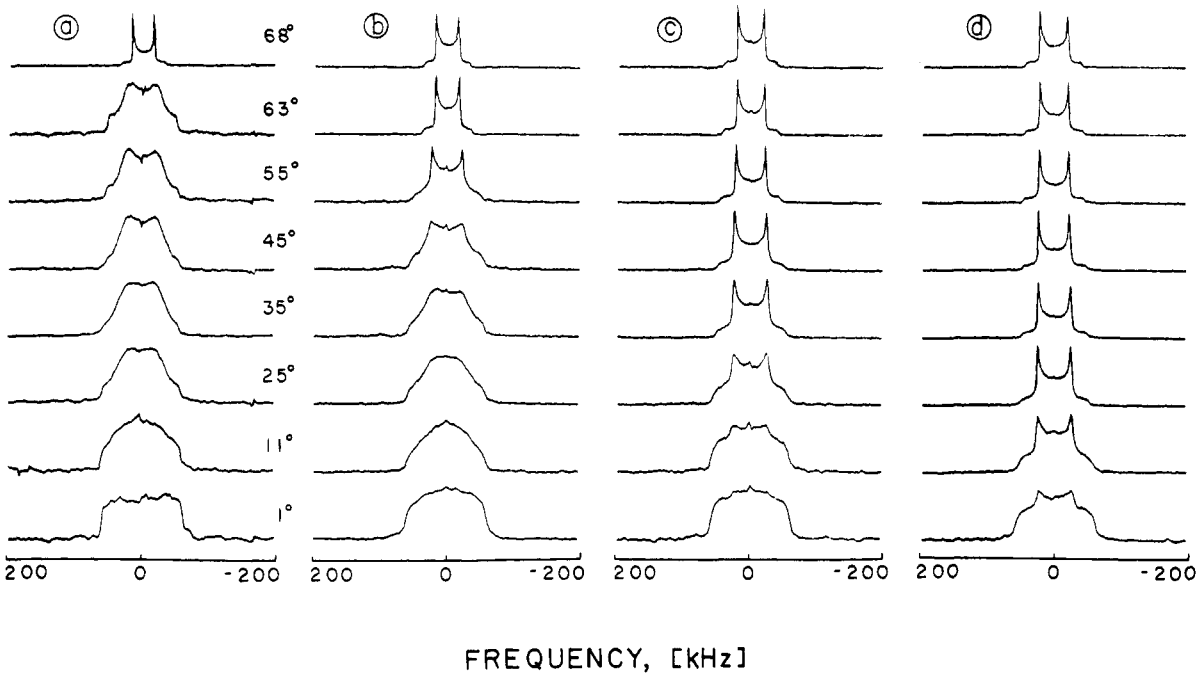

FIGURE 4: ^2H NMR spectra of 2[4,4-$^2H_2$]DPPE as a function of temperature: (a) 0, (b) 10, (c) 30, and (d) 50 mol % CHOL, respectively.

observed. Below about 25 °C the head group ^2H spectra broaden, but they do not become significantly wider. This is illustrated in Figure 9b where we show the full width of this line at half-height vs. mole percent CHOL. Note that the widths are about 17–23 kHz, which are about the same as the separation of the *parallel* edges of the sharp axially symmetric spectra (16–19 kHz). As will be discussed below, these results suggest that CHOL has relatively little effect on the conformation of the DPPE head group. However, the dynamic properties of the head group do change with temperature and CHOL concentration.

Discussion

(A) ^{13}C Spectra of DPPE/CHOL Mixtures. ^{13}C NMR spectra of *sn*-2 $^{13}C{=}O$ labeled phospholipids have proven useful in studies of the phase behavior and equilibria in pure and mixed lipid systems. In the gel state the spectrum of this label consist of an axially symmetric powder pattern, which collapses to an isotropic-like line in the liquid-crystalline phase (Wittebort et al., 1981, 1982; Blume et al., 1982a). This is illustrated in Figure 1a for pure 2[1-^{13}C]DPPE. The reason for this behavior is a change in the orientation of the unique axis of the ^{13}C shielding tensor, with respect to the molecular director, from an angle θ in the L_β phase to an angle $\theta \simeq 54.7°$ in the L_α phase. As discussed previously (Wittebort et al., 1982), the angle θ may be obtained from the formula

$$\Delta\sigma^R = \Delta\sigma^{RL}\overline{(1/2)(3\cos^2\theta - 1)} \quad (1)$$

where $\Delta\sigma^R$ is the rotationally averaged breadth of the tensor, $\Delta\sigma^{RL}$ is the breadth of the rigid lattice tensor, which is assumed to be axially symmetric, and the bar denotes a time-averaged quantity. For DPPE in the L_α phase $\theta \simeq 28°$. There is

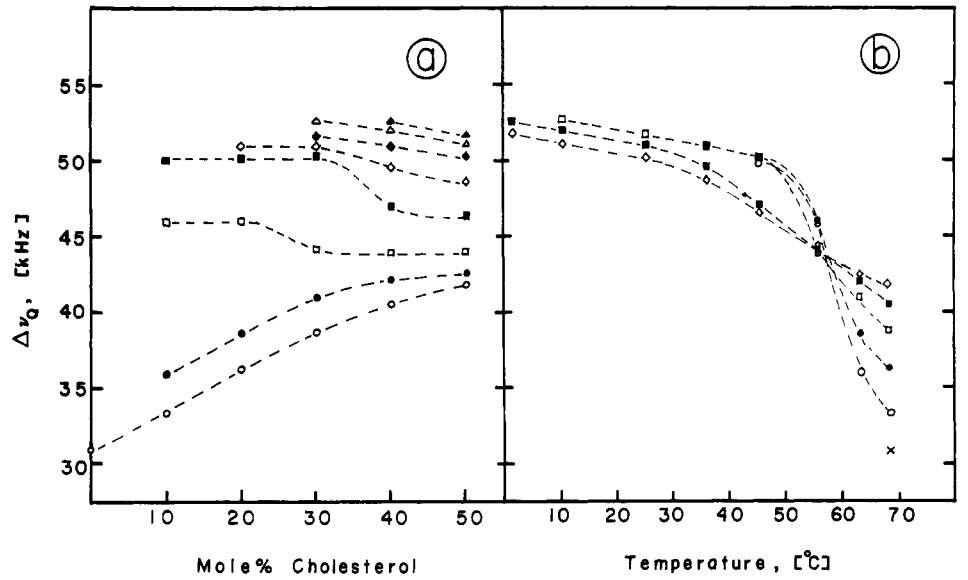

FIGURE 5: Residual quadrupole splitting $\Delta\nu_{Q\perp}$ for 2[4,4-$^2H_2$]DPPE/CHOL mixtures. (a) Vs. CHOL content: (○) 68 °C, (●) 63 °C, (□) 55 °C, (■) 45 °C, (◇) 35 °C, (◆) 25 °C, (△) 11 °C, and (▲) 1 °C. (b) Vs. temperature: (×) 0, (○) 10, (●) 20, (□) 30, (■) 40, and (◇) 50 mol % CHOL, respectively.

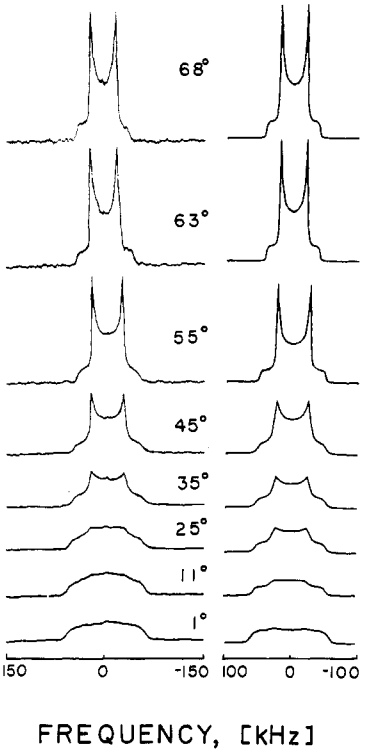

FIGURE 6: (Left) ^2H NMR spectra of a mixture of 2[4,4-$^2H_2$]DPPE with 20 mol % CHOL as a function of temperature. (Right) Lineshape simulations using data derived from the simulations of the ^{13}C NMR spectra in Figure 1. (For further explanation of model, see text.) The experimental spectra and the simulations are plotted scaled to the absolute intensity of the quadrupole echo.

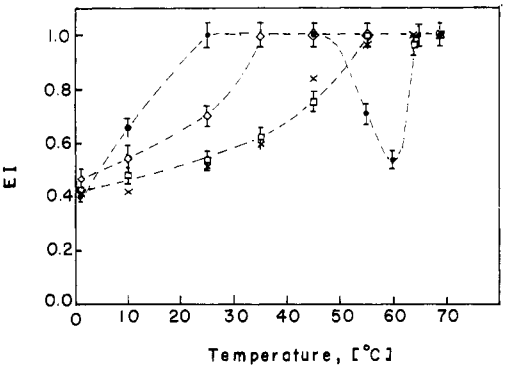

FIGURE 7: Normalized experimental quadrupole echo intensities for (●) pure 2[4,4-$^2H_2$]DPPE, (□) 2[4,4-$^2H_2$]DPPE/20 mol % CHOL, and (◇) 2[4,4-$^2H_2$]DPPE/40 mol % CHOL, respectively. (×) Calculated echo intensities for sample with 20 mol % CHOL as shown in Figure 6. The error bars denote typical uncertainties in the measurements of the absolute echo intensities.

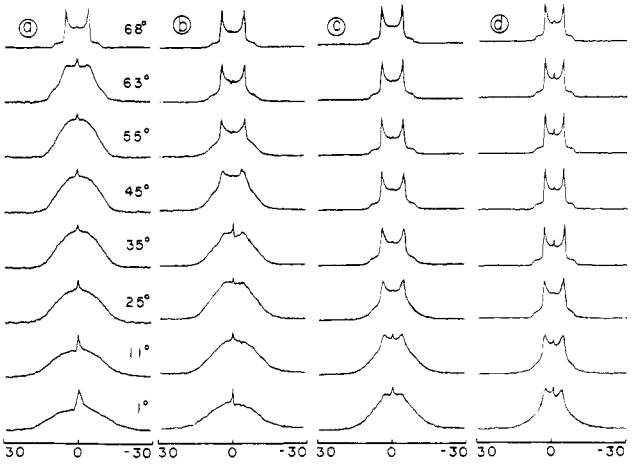

FIGURE 8: ^2H NMR spectra of $^+NH_3$–CH_2–CD_2–DPPE/cholesterol mixtures: (a) 0, (b) 10, (c) 30, and (d) 50 mol % CHOL, respectively.

considerable evidence that a conformational change at the *sn*-2 C=O is responsible for the rather dramatic alteration in ^{13}C spectra observed at the phase transition. Specifically, we believe that the C_1–C_2 bond of the glycerol backbone changes from a gauche conformation in the L_β phase to an unspecified but different average conformation in the L_α phase. Accompanying this conformational change is a conformational change at the *sn*-2 carbonyl, which results in the collapse of the ^{13}C=O powder pattern (Blume et al., 1982a). The ^{13}C spectra in parts b–f of Figure 1 show that the addition of CHOL to the DPPE bilayer also induces this conformational change. Furthermore, the change begins, and is complete, at lower temperatures as the CHOL concentration is increased.

It is known from DSC studies of the DPPE/CHOL system that addition of CHOL to pure DPPE broadens the phase

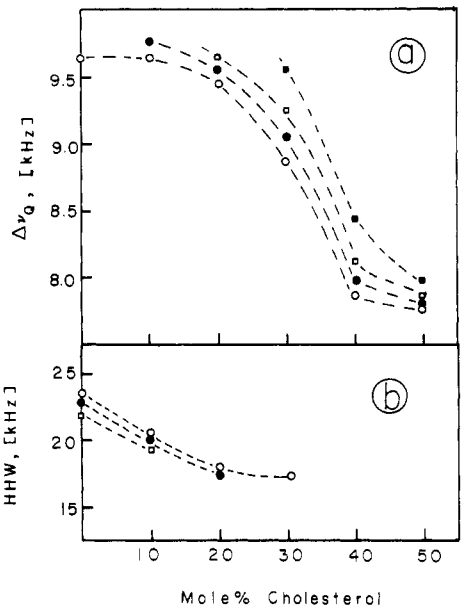

FIGURE 9: (a) Residual quadrupole splitting $\Delta\nu_{Q\perp}$ for $^+NH_3$–CH_2–CD_2–DPPE/CHOL mixtures: (○) 68 °C, (●) 63 °C, (□) 55 °C, and (■) 45 °C. (b) Full width at half-height of the broad component vs. CHOL content: (○) 1 °C, (●) 11 °C, and (□) 25 °C.

transition, lowers the transition enthalpy, and abolishes the endotherm when 50 mol % CHOL is reached (Blume, 1980). In addition, the onset of melting is continuously shifted to lower temperatures. The features of the *sn*-2 $^{13}C{=}O$ spectra of Figure 1 are in general agreement with these DSC results. Specifically, the appearance of the sharp component in the spectra suggests the presence of fluid lipids at progressively lower temperatures. However, the DSC experiments also reveal a sharp component in the endotherm of DPPE/CHOL mixtures that is approximately unshifted from that observed for pure DPPE. Inside this calorimetric endotherm, and well before the completion of melting, the *sn*-2 $^{13}C{=}O$ spectra consist of the single L_α-like line. We will discuss this point further below.

A second interesting feature of the spectra of Figure 1 is the fact that for a given CHOL concentration, there invariably exists a temperature region over which a two-component spectrum is observed; for example, at 20 mol % CHOL the two-component line shape is observed from about 11 °C up to 45 °C. Furthermore, when the two components are present, both are broadened due to chemical exchange (lateral diffusion); the broadening is most noticeable in the sharp component of the spectra. The observation of these line shapes is clear evidence for the coexistence of two conformationally inequivalent molecules in the DPPE/CHOL bilayer, one of which is gel-like and the other has properties of L_α-phase lipids. The computer simulations adjacent to the experimental spectra permit us to extract the fraction of each type and the associated exchange rate. In performing these simulations we have used what is essentially a two-parameter model. Specifically the rigid lattice tensor values and their orientations with respect to the diffusion axis one assumed to be known. Furthermore, it assumed that the axially diffusion rates are fast on the ^{13}C time scale. The parameters that are adjusted in order to reproduce the line shape are then the fractional population of the sharp L_α-like component, f_F, and the exchange rate. As is evident from Figure 1 this model results in very good reproductions of the experimental line shapes. Its success indicates that the lateral separation between the conformationally inequivalent species is small and the translational diffusion constants are sufficiently large, so that all molecules exchange with the same effective rate.

An estimate of the distance of separation of the two components may be obtained from the relation between the translational diffusion constant, D_T, and the mean square displacement, $\bar{x}^2$:

$$\bar{x}^2 = 4D_T t \qquad (2)$$

The exchange rates, R_{ex}, are about 500 s^{-1} (see Figure 3), which leads to an intermediate exchange lifetime of 2×10^{-3} s. Taking a value of 1×10^{-10} cm^2/s for D_T (Rubenstein et al., 1979) yields a mean square displacement of about 8×10^3 $Å^2$. This corresponds to an area occupied by roughly 150 lipid molecules, and thus the conformationally inequivalent species are fairly close together. It should be mentioned that this type of model also reproduces the *sn*-2 $^{13}C{=}O$ spectra observed from pure lecithins in the $P_{\beta'}$ pretransition region. However, these two systems apparently are quite different from binary DPPC/DPPE mixtures. In the two-phase region of this mixture, the ^{13}C spectra are qualitatively similar in appearance, e.g., a narrow L_α-like line superimposed on an L_β powder pattern, but the line shapes cannot be accurately reproduced unless a distribution of exchange rates is introduced. We believe this reflects the presence of larger domain sizes in the DPPC/DPPE system, and lipids in the centers of the domains do not "exchange" at the same rate as those near a boundary. Indeed, Hui (1981) has observed domains with diameters up to 0.5 μm (2×10^7 $Å^2$) in PC/PE and PS/PC mixtures. This domain size is clearly much larger than that estimated above for DPPE/CHOL mixtures, and thus serves as one means to understand the differences in the $^{13}C{=}O$ NMR spectra.

In the above discussion, we have referred to the sharp component in the two-component ^{13}C spectra as being an L_α-like spectrum. The origin of this terminology derives from the fact that this component alone is seen in the L_α phase of pure DPPE and lecithins, whereas the broad axially symmetric powder pattern is observed in the L_β phase of DPPE and the $L_{\beta'}$ phase of lecithins. Moreover, we will see below that the appearance of the sharp component in the ^{13}C spectra does coincide with the appearance of a sharp axially symmetric component in the ^2H acyl chain and head group spectra. Because of these independent spectral measurements, it is clear that the DPPE/CHOL bilayers do have some molecules with some L_α-phase properties in the temperature composition region where the two-component ^{13}C spectrum is observed. Moreover, for this reason we associate the intensity of the sharp component in the ^{13}C spectra with the fraction of fluid molecules, f_F. This quantity is obtained directly from the simulations of the ^{13}C spectra in Figure 1 and is plotted as a function of temperature and CHOL concentration in Figure 2.

The curves in Figure 2a, which show f_F as function of temperature at various CHOL concentrations, show no discontinuities and are not sigmoidal in shape. This observation therefore suggests a gradual, continuous transformation of gel-like to liquid-like molecules, with increasing temperature. Moreover, at higher CHOL concentrations the transformation begins and is complete at progressively lower temperatures. The curves of Figure 2a can be extrapolated to $f_F = 1$ to obtain the temperature corresponding to the disappearance of the gel-state powder pattern. These temperatures are 61, 58, 51, 37, and 30 °C for the 10–50% CHOL concentrations, respectively. Similar data may be obtained from Figure 2b, and we find at 34, 45, and 55 °C that $f_F = 1$ at 42, 33, and 26% CHOL, respectively. These data will be used below in construction of a temperature–composition diagram. In addition,

it should be possible to obtain the temperatures for the initial appearances of the sharp L_α-like line by extrapolating the plots in Figure 2a to $f_F = 0$, and some of the curves yield $f_F = 0$ 15–25° below 0 °C. Below 0 °C we have found, however, that the axially symmetric powder pattern begins to broaden and at about −15 °C the sharp L_α-like line is no longer observed. It seems probable that these effects are due to water freezing, and therefore, these extrapolations are of questionable validity. The estimated errors in f_F are ±0.1 in regions where $f_F \leq 0.2$ or ≥ 0.8 and ±0.05 between these limits. For clarity we have omitted error bars in the plots of Figure 2.

Also included in Figure 2a are the integrated and normalized heat capacity curves obtained from DSC studies of DPPE/CHOL mixtures. These curves show that the temperature for the onset of melting, T_{onset}, is continuously shifted to lower temperature with increasing CHOL concentration, while the temperature for the completion of melting, T_{comp}, remains approximately unchanged. Note also that for a given CHOL concentration, f_F becomes nonzero 10–20 °C below T_{onset} and generally approaches unity before T_{comp}. In other words, the axially symmetric gel-state spectrum transforms to the single narrow L_α-like line well before the peak of the DSC endotherm is reached. Thus, the ^{13}C NMR and DSC experiments are clearly reporting different phenomena. The differences between the calorimetric and the NMR results can be understood when the basic differences between the two methods are considered.

Scanning calorimetry, at least when the normal experimental procedure is used and dilute suspensions are analyzed, is only able to detect a *cooperative* transition. The transition can be either a first-order transition, connected with a true latent heat of melting, or a second-order transition with an apparent heat of melting. In both cases a transition enthalpy can be determined from the heat capacity vs. temperature curve. Any noncooperative change in the heat capacity is usually hidden in the base line, which might show a slight slope or change in slope due to this process. In contrast, NMR experiments are able to monitor both types of behavior, cooperative as well as noncooperative. The onset of melting observed by calorimetry thus only indicates the beginning of a cooperative process. The system below this temperature may well be in a state of partial disorder, as indicated by the presence of a considerable amount of "liquid"-like line in the ^{13}C spectrum. At the same time, the presence of only one line in the NMR spectrum at higher temperature does not necessarily mean that the state of the system does not change with increasing temperature. It might appear liquid when only the $^{13}C{=}O$ resonance is observed, but it could still show considerable changes in molecular properties when other parts of the molecule are considered. In fact a careful inspection of the line width of the ^{13}C resonance reveals that it decreases with temperature. For instance, in the sample with 40% cholesterol, it changes from 350 Hz at 35 °C to 220 Hz at 65 °C, which suggests that the dynamic and/or structural properties of the system are not constant. We see below that the ^2H NMR spectra of 2[4,4-$^2H_2$]DPPE show a similar, but much more obvious, narrowing.

It should also be mentioned that the binary DPPC/DPPE system exhibits a quite different behavior than is illustrated in Figure 2a for DPPE/CHOL. In this particular system T_{onset} and T_{comp} coincide with the first appearance of sharp component in the ^{13}C spectra and the disappearance of gel-state powder pattern, respectively. In addition, the f_F vs. T plots and the integrated DSC curves are reasonable facsimiles of one another. The differences observed in the two mixtures probably arise from microscopic structural differences. For example, the larger domains that exist in the DPPC/DPPE mixture are likely due in part to the structural similarities between the two molecules—e.g., they differ only in the presence or absence of three CH_3's at the N-terminal part of the head group. Thus, insertion of a DPPC molecule into a DPPE lattice is not expected to be a larger perturbation. For similar reasons it is not surprising that the conformational change at the *sn*-2 C=O occurs at the same temperature and composition at which the acyl chains begin to disorder—e.g., a narrow axially symmetric pattern is seen in ^2H acyl chain spectra. Furthermore, the processes are reasonably cooperative, and thus the f_F vs. T plots and the DSC results coincide.

In contrast, CHOL is structurally quite different from DPPE and would be expected to perturb the DPPE lattice, but in two slightly different ways. In the glycerol backbone/head group region of DPPE, CHOL could be viewed as a spacer. Insertion of the steroid into the lattice would thus be similar to the lateral expansion observed in traversing the $L_\beta \rightarrow L_\alpha$ phase transition. Thus, if CHOL disrupts the molecular packing present in the head group region of pure DPPE, it might also induce a conformational change similar to that observed at the main transition. On the other hand, the presence of the rigid steroid ring system could have the opposite effect on the acyl chains. In particular, it could suppress gauche–trans isomerization, and the melting of the acyl chains would take place over a rather wide temperature range and would thus appear to be less cooperative. For these reasons it appears reasonable that the f_F vs. T plots obtained from the ^{13}C data would not mimic the integrated DSC curves. These rather straightforward chemical ideas provide one means to understand the differences between the behavior of the DPPC/DPPE system and that illustrated in Figure 2a for DPPE/CHOL. As will be seen below, they seem to be borne out by the temperature and composition dependence of the acyl chain spectra.

One of the most interesting questions concerning PC/CHOL mixtures concerns the existence of a vertical phase boundary at 20 mol % CHOL. The presence of such a phase boundary was suggested sometime ago by Shimshick & McConnell (1973) and has subsequently been the subject of numerous investigations [see, for example, Recktenwald & McConnell (1981) and references therein]. According to these models the presence of the $P_{\beta'}$ phase seems to be a requisite for this phase boundary, where pure PC is in equilibrium with a PC/20% CHOL mixture. The ^{13}C spectra of Figure 1 permit us to investigate the existence of such phase boundaries in the DPPE/CHOL system. Specifically for a given temperature, an increase in the CHOL concentration should result in an increase in f_F. Moreover, if a vertical phase boundary is traversed, and the system became significantly more liquid-like, then it is possible that a discontinuity in f_F would be observed and the parameter might approach unity. It is for this reason that we also show f_F data obtained from the ^{13}C spectra as a function of CHOL content in Figure 2b. Inspection of the figure shows that with experimental error, the curves are slightly sigmoidal in shape at 1, 11, 23, and 34 °C. Moreover, the midpoints of the sigmoidal parts of these curves all occur at about 25 mol % CHOL, which could be interpreted as evidence for the presence of a vertical phase boundary. Note, however, that for CHOL concentration >25%, we still observe the axially symmetric powder pattern characteristic of gel-phase lipids (in Figure 1), and therefore $f_F < 1$. Moreover, it will be seen below that the ^2H acyl chain and head group spectra appear to be a superposition due to gel and fluid lipids.

Thus, the molecular event(s) that lead to the sigmoidal curves in Figure 2b do not correspond to the complete conversion of gel lipid to either fluid or liquid-crystalline lipid. At higher temperature, 45 and 55 °C, we do not resolve these breaks since $f_F \simeq 1$. In addition, it will be seen below that points at 30% CHOL and higher in the 23 °C curve correspond to temperatures and compositions inside the calorimetrically observed transition. For this reason additional cooperatively melted DPPE probably contributes to f_F and enhances the sigmoidal shapes of the curves.

The other quantity that can be derived from the ^{13}C spectra of Figure 1, which is relevant to this discussion, is the exchange rate between the gel- and fluid-like fractions. These data are shown in Figure 3a,b, and as expected, R_{ex} increases with temperature, and plots of ln R_{ex} vs. $1/T$ (not shown) yield straight lines in the low-temperature region. However, deviations from linearity are observed at higher temperatures and coincide with temperatures inside the calorimetric endotherm. This is not surprising because the exchange rates are approaching the fast limit on the ^{13}C time scale, the fraction of gel-like component is becoming small, and as a result the values for R_{ex} obtained from the simulations are not very accurate. The plots of R_{ex} vs. CHOL content in Figure 3b are similar to the plots of f_F in Figure 2b insofar as they show sigmoidal behavior at low temperature. At higher temperatures (35–55 °C) there is a large increase in R_{ex} above 20% CHOL, for example, at 35 and 45 °C. This type of behavior is reminiscent of that observed in photobleaching experiments in PC/CHOL mixtures (Rubinstein et al., 1979). However, we should point out that the increase in R_{ex} amounts to a factor of about 2, whereas in the photobleaching experiments the translational diffusion constants increase by 1–2 orders of magnitude. At higher temperatures the increase in R_{ex} is larger, but as mentioned above, the large exchange rates, which determine the shapes of these curves, correspond to regions where cooperative melting of the acyl chains is observed.

Another effect that might contribute to the sigmoidal shapes of these curves is that in samples containing greater than 30% CHOL we have observed a metastable behavior. In particular, when 40% and 50% CHOL/DPPE samples are stored at reduced temperature for prolonged periods, we have found that they yield NMR spectra similar to those seen for the 30% sample. Heating these samples to temperatures above 25 °C apparently redissolves the CHOL. These observations will be discussed in more detail below, but they suggest strong nonideal mixing at CHOL concentrations greater than 30%. It is possible that this could also suppress the f_F values shown in Figure 2b, and thus contribute to the sigmoidal shapes of the curves.

In summary, the ^{13}C spectra indicate that at temperatures below 34 °C, and at CHOL concentrations between 20 and 30%, some changes occur in DPPE/CHOL bilayers that lead to a sigmoidal increase in f_F and R_{ex}. At higher CHOL concentrations a fraction of gel-like DPPE molecules remains, and the population of this fraction decreases with either increasing CHOL content or temperature. These observations appear to exclude the possibility of a two-phase mixture of DPPE/~25% CHOL and CHOL since the ^{13}C spectra would presumably consist of a single line. They are perhaps explanable in terms of a "percolation effect" as recently described by Snyder & Freire (1980). In this context the fraction of fluid lipid would continue to increase after the system becomes connected, and this is the effect we observe. Nevertheless, we should remind the reader that the spin-label and photobleaching experiments, which provide the experimental evidence for the boundary at 20% CHOL, were performed for PC/CHOL mixtures and the calculations of Snyder & Freire were concerned with sphingomyelin/CHOL and PC/CHOL mixtures. There may or may not be a direct correspondence between these results and those reported here for DPPE/CHOL mixtures. Finally, a third factor that could contribute to the sigmoidal shapes of the curves is the metastable behavior to be discussed further below.

(B) ^2H Spectra of 2[4,4-$^2H_2$]DPPE/CHOL Mixtures. The *sn*-2 $^{13}C{=}O$ spectra discussed above are very informative. Nevertheless, when taken alone, they furnish an incomplete picture of the dynamic and structural changes that occur in phospholipid/CHOL mixtures as a function of temperature and composition. For example, it has been known for sometime that CHOL produces a condensing effect in liquid-crystalline-like monolayers, whereas the opposite effect is seen in condensed, gel-like systems—e.g., they are "fluidized" (Shah & Schulman, 1967; Phillips, 1972; Müller-Landau & Caden head, 1979; Melchior et al., 1980). Another commonly employed description of the effect is that CHOL orders the liquid-crystalline phase, but disorders the gel phase. One aspect of the disordering or fluidization of the gel phase of DPPE can clearly be examined with the ^{13}C spectra of Figure 1, specifically, the conformational change in the glycerol backbone. However, since these spectra collapse to a narrow line in the fluid-like phases, they are not very useful for studying the condensing effect of CHOL. Furthermore, the observation that the *sn*-2 $^{13}C{=}O$ spectra invariably consist of a narrow line suggests that any CHOL-induced condensation of the lipid lattice does not involve the glycerol backbone region. In fact the ^2H spectra of 2[4,4-$^2H_2$]DPPE show that the condensing effect of CHOL involves the suppression of gauche–trans isomerization in the acyl chains.

In Figure 4 we show ^2H NMR spectra of pure 2[4,4-$^2H_2$]DPPE and of mixtures containing 10, 30, and 50% CHOL as a function of temperature. In the L_β phase of pure DPPE, the ^2H spectra are broad powder patterns and can be simulated with a model that assumes an approximately all-trans chain that diffuses about its long axis with a 3-fold jump rate of about 7×10^5 s^{-1} just below the T_c (Blume et al., 1982a). The fact that the chain is approximately all-trans follows from the observation that the total breadth of the gel-state spectra is 115 kHz at 25 °C, and decreases to 110 kHz at at 55 °C. These breadths are close to the value of 125 kHz expected from a strictly all-trans conformation. At the phase transition the ^2H spectrum narrows by about a factor of 2 and sharpens considerably. These two spectral changes are due to increased rates of gauche–trans isomerization and rotational diffusion. In a quadrupole echo experiment, fast-limit spectra are obtained for a CD_2 group when the rates are $>10^7$ s^{-1}. The observation of the sharp spectrum above T_c suggests that the isomerization and axial diffusion rates at least satisfy this condition and may well be faster.

Addition of CHOL to DPPE results in two types of changes in the ^2H chain spectra. First, at temperatures above T_c of the pure lipid, the breadth of the L_α phase powder pattern is increased. This increase is apparent in the 68 °C spectra of Figure 4 and is also illustrated in Figure 5a, where we have plotted $\Delta\nu_{Q\perp}$ vs. mole percent CHOL. Here it can be seen that $\Delta\nu_{Q\perp}$ changes from about 31 kHz in pure DPPE to 42 kHz at 50 mol % CHOL. This marked increase illustrates the condensing effect of CHOL. It will be shown elsewhere (Wittebort et al., 1982) that the breadth of an L_α phase ^2H spectrum is directly proportional to the population of trans

CD_2 segments at a particular chain position. In the context of this model, the observed increase in $\Delta\nu_{Q\perp}$ is then indicative of increased trans population at the 4 position, or a more ordered chain. Correspondingly, the average cross-sectional area required for a DPPE molecule is lower, and thus the bilayer is "condensed".

Another feature of the $\Delta\nu_{Q\perp}$ vs. T curve at 68 °C is that it shows no breakpoints or discontinuities, which suggests the absence of phase boundaries at these temperatures and compositions. This behavior is quite different from that observed for DPPC/CHOL and DMPC/CHOL (Haberkorn et al., 1977; Jacobs & Oldfield, 1979) where the quadrupole splittings first increase with addition of CHOL, and then either level off or decrease slightly. On a microscopic scale, the increase of $\Delta\nu_{Q\perp}$ with CHOL in DPPE and in PC can be explained by invoking fast exchange between an L_α-like fraction of lipids and an ordered fraction, presumably lipids residing adjacent to CHOL in the bilayer. Since only a single averaged quadrupole splitting is observed, the lifetimes must be short enough to satisfy fast-exchange conditions.

At lower temperatures we observed a second and distinctly different type of CHOL-induced effect in the acyl chain spectra. Inspection of the spectra of Figure 4 shows that at sufficiently low temperatures a gel-state spectrum is observed, but that a sharp axially symmetric component appears as the temperature is increased. This is most easily discerned in the 10 mol % CHOL sample where the gel-state powder line shape is evident between 1 and 45 °C, and transforms to a sharp axially symmetric spectrum for $T \geq 45$ °C. At 30 and 50% CHOL the sharp component is evident at lower temperatures, and we have plotted $\Delta\nu_{Q\perp}$ for this component vs. mole percent CHOL in Figure 5a. For all temperatures below 55 °C, it can be seen that $\Delta\nu_{Q\perp}$ decreases with increasing CHOL content. At 55 °C the decrease appears to be sigmoidal, between 20 and 30%, and at 45 °C between 30 and 40% CHOL, whereas at lower temperatures only a negative slope is observed in the plots. However, it is clear from the curves that CHOL has an effect that is opposite to that observed above T_c of the pure lipid, and it could be said that indeed CHOL does "disorder" a gel-state DPPE bilayer. Nevertheless, the curves in Figure 5a show that the disordering effect is certainly not large. For example, the largest change in the $\Delta\nu_{Q\perp}$ vs. CHOL plots occurs at 45 °C and amounts to a narrowing from 50 kHz to about 46 kHz at 50% CHOL. Furthermore, at lower temperatures, and even at high CHOL concentrations, the spectral width approaches that seen in the gel state of pure DPPE. For example, at 25 °C and 30 mol % CHOL the total spectral width is 104 kHz ($\Delta\nu_{Q\perp}$ = 52 kHz) as compared to a 115-kHz width observed in pure DPPE bilayers. As discussed above these large spectral splittings are indicative of large trans populations in the acyl chains. It therefore follows that in these temperature–composition regions the predominant molecular effect of CHOL, at least at the 4 position of the *sn*-2 chain, is not to disorder the chains. Instead, they are reasonably well-ordered, and the addition of CHOL simply disrupts the lattice and permits the DPPE molecules to diffuse more freely about their long axes.

In Figure 5b we have plotted the $\Delta\nu_{Q\perp}$ data vs. temperature, and this plot illustrates the point more clearly. In addition, these curves indicate that the DPPE acyl chains do disorder at higher temperature, and they also explain the sigmoidal shapes of the $\Delta\nu_{Q\perp}$ vs. mole percent CHOL plots (Figure 5a) at 45 and 55 °C. In the low-temperature region of Figure 5b the 30, 40, and 50% CHOL samples show the large quadrupole splittings expected of an approximately all-trans chain. As the temperature is increased, the splittings from these high CHOL content samples decrease approximately linearly until about 40–50 °C, where they begin a rapid decline to the values observed at 68 °C. Furthermore, at these temperatures the sharp axially symmetric components appear in the ^2H spectra of the 10 and 20% CHOL samples, and these splittings also decrease precipitously with further increases in temperature. The curves for these latter two samples and the 30% CHOL sample are sigmoidal in shape, and interesting enough, the midpoints of these curves coincide with the midpoints of the integrated heat capacity curves in Figure 2a. Thus, the chain disordering illustrated in Figure 5b and the sharp, unshifted component observed in the DSC traces of DPPE/CHOL mixtures coincide. The clear association of these two phenomena permits a microscopic interpretation of the DSC experiment; specifically, the sharp, roughly unshifted component observed in the DSC traces represents a cooperative transition of the acyl chains to a higher degree of disorder. Furthermore, these results emphasize that the association of a sharply axially symmetric ^2H spectrum with a liquid-crystalline phase must be done with care. *In particular, the observation of such a spectrum is a necessary condition for liquid-crystalline behavior, but, since cooperative changes to higher degrees of disorder are still possible, it is clearly not always a sufficient condition.*

Under Results we stated that we believed that the ^2H chain labeled spectra shown in Figure 4 consist of two components, and we are now in a position to examine this statement more carefully. There are at least two reasons to suspect that this might be the case. First, a careful inspection of the ^2H line shapes at high CHOL concentration and low temperatures reveals some line shapes that might be interpreted as consisting of two components. For example, at 30% CHOL and 11 °C and at 50% CHOL and 1 °C we have recorded what are nearly identical line shapes that appear to consist of a sharp axially symmetric spectrum superimposed on a flat-topped gel-state spectrum. Second, the *sn*-2 $^{13}C{=}O$ spectra clearly show the presence of two components at many temperatures, and more importantly, at the two temperatures and CHOL concentrations mentioned above, the ^{13}C spectra are also replicas of one another. Thus, the fraction of molecules that contributes to the sharp line in the *sn*-2 C=O spectra appears to be related to the fraction that results in the sharp component seen in the ^2H spectra. A corollary of this statement is that for a given CHOL concentration, the sharp components should appear in the ^{13}C and ^2H spectra at the same temperatures, and in certain cases this is observed. For example, at 20 mol % CHOL we first observed the sharp component in the ^{13}C spectra at 11 °C, and the same is (barely) true for the ^2H spectra illustrated in Figure 6. Nevertheless, in other cases this association is less obvious. In the 10 mol % sample the sharp component begins to develop in the ^{13}C spectra at 23 °C, but the ^2H spectra of this sample are nearly identical with those seen for pure 2[4,4-$^2H_2$]DPPE, until we reach 45 °C, where they perceptibly begin to differ. We should note, however, that this is not an unexpected result since, as is shown in Figure 5b, the quadrupole splittings are approaching those for pure DPPE. At 25 °C there is an approximately linear increase in $\Delta\nu_{Q\perp}$ with decreasing CHOL content of 1.25 kHz/10% CHOL. Thus, at 10 mol % CHOL we would expect a splitting of about 54 kHz and a total spectral breadth of 108 kHz. The width of the pure DPPE spectrum at this temperature is 115 kHz, and there is exchange between the two components at rates of $\sim 5 \times 10^2$ s^{-1}, which will broaden the line shapes. Under these circumstances it would be surprising

if in fact two well-resolved components were visible in the ^2H spectra. Nevertheless, these observations are strongly suggestive of the presence of two components in the ^2H spectra of 2[4,4-$^2H_2$]DPPE/CHOL mixtures. Furthermore, they indicate that it should be possible to simulate the ^2H spectra by using data obtained from the ^{13}C spectra—specifically, f_F and R_{ex}.

In Figure 6 we show experimental spectra obtained from 2[4,4-$^2H_2$]DPPE/20% CHOL together with simulations obtained with a model that is similar to that employed in the ^{13}C spectral simulations of Figure 1. In particular, we assume two components, one of which has the 3-fold axial diffusion rates observed for pure DPPE at the appropriate temperature (Blume et al., 1982a). For the second fluid-like component, we have assumed fast 3-fold axial diffusion, and have tilted the chain at an angle with respect to the diffusion axis in order to match the splitting observed for the sharp component of the spectrum. The fractional population of each of these components and the exchange rates between the components were those obtained from the ^{13}C spectra of Figure 1. As can be seen from Figure 6, there is good agreement between the simulations and the experimental results. Note in particular that the line shapes are reproduced well, and that there is a conspicuous absence of two well-resolved splittings in any of the spectra. For instance, at 35–45 °C the ^{13}C spectra show that about 0.5–0.75 of the DPPE is fluid and exhibits a quadrupole splitting of ~50 kHz. When this exchanges with gel-like lipid the result is simply a broadening of the spectrum.

In addition, we have plotted the spectra of Figure 6 on an absolute intensity scale, which provides additional evidence for exchange between two components. In particular, both intra- and intermolecular slow motions will reduce the quadrupole echo intensity (Spiess & Sillescu, 1981), and therefore, the reproduction of the absolute intensity of the spectra is an additional constraint that the simulations must satisfy. The point is further illustrated in Figure 7 where we have plotted the normalized echo intensities as a function of temperature for three different samples. In pure 2[4,4-$^2H_2$]DPPE two temperature regions with low-echo intensities can be distinguished. Below 25 °C intermediate regime axial diffusion rates are responsible for the reductions in intensity, while at temperatures near the main phase transition exchange processes between liquid-crystalline and gel-state domains, as well as internal motions, contribute to the intensity decline. In samples containing CHOL the reduction is dispersed over a wider temperature range, which reflects the gradual transformation from gel- to liquid-crystalline-type behavior. In addition, at a given temperature—e.g., 25 °C—a higher CHOL concentration increases the intensity because, first, the fraction of gel-like molecules has decreased and, second, the exchange processes are faster. Note the good agreement between the experimental and calculated echo intensities for the DPPE/20% CHOL sample.

The model we have employed for the simulations of Figure 6 is certainly a simplification of the real situation. For example, we have accounted for the observed splittings by adjusting the angle between the C–D vector and the molecular long axis, when in fact the narrowing is probably due to higher populations of gauche isomers. Inclusion of these processes, particularly for the slow-rotating component, would probably improve the simulations as the intensity in the middle of the spectrum would be increased (see, for instance, the 25 °C spectrum). However, even with this relatively simple model the major effects are predicted with reasonable accuracy. These results also emphasize a major deficiency of the ^2H experiment in this type of system. Specifically, the folding of the two transitions of the $I = 1$ powder spectrum, the presence of two nearly identical quadrupole splittings, the existence of rather small domains in the DPPE/CHOL system, and quadrupole echo distortions conspire to lead to spectra that do not exhibit two components in an obvious way. Thus, if we had confined our investigations to ^2H spectroscopy, then we would most likely have drawn incorrect conclusions. It is obviously important in this type of investigation to perform multiple measurements in order to properly dissect the various effects that are present.

It should be mentioned that ^2H acyl chain spectra of other systems exhibit some features that are similar to those described here for DPPE/CHOL. Maraviglia et al. (1982) have employed phospholipid exchange protein to label red blood cells with [$^2H_{62}$]DPPC (DPPC with both acyl chains perdeuterated) and have examined the temperature dependence of the spectra. The residual quadrupole splittings range from about 56 kHz at 5 °C to 41 kHz, at 45 °C, which is similar to what is observed for DPPE/CHOL mixtures at high (40–50%) CHOL contents. In addition DPPC/CHOL mixtures at low CHOL contents yield $\Delta\nu_{Q\perp}$ vs. T curves with a sigmoidal break, whereas at high CHOL concentrations the plots become almost linear (T-H. Huang, R. J. Wittebort and R. G. Griffin, unpublished results). The observation of these effects in these two model systems, and in one biological membrane, suggests that the behavior illustrated in Figure 5 may be a common feature of glycerophospholipid/CHOL mixtures. Finally, the spectra illustrated in Figure 6 may be of some importance to ^2H NMR studies of reconstituted lipid/protein mixtures (Rice et al., 1979; Kang et al., 1979; Paddy et al., 1981; Seelig et al., 1981). For example, in the case of 1[6,6-$^2H_2$]POPC/cytochrome oxidase mixtures the presence of the protein results in a broadening of the spectra and noticeably lower signal-to-noise ratios than are seen in spectra of the pure lipid. Thus, it seems possible that chemical exchange between free and "boundary" lipids could possibly be responsible for the spectral line shapes observed in reconstituted systems. This possibility has recently been discussed by Paddy et al. (1981) and Bienvenue et al. (1982). The results in Figure 6 suggest that unless the ^2H spectra of the "free" and boundary lipids are quite different *and* the exchange between the two species is slow, it will be difficult to resolve spectra from these two species with ^2H NMR.

(C) ^2H Spectra of Head Group Labeled DPPE. We have suggested above that the CHOL-induced appearance of the sharp components in the *sn*-2 $^{13}C{=}O$ and 2[4,4-$^2H_2$]DPPE spectra may be related to disruption of a hydrogen bonding network in the head group region. Concurrently, there is a conformational change at the *sn*-2 C=O and the onset of relatively fast axial diffusion of the DPPE molecules, which result in sharp components in these spectra. Obviously, this hypothesis can be tested by examining head group labeled DPPE and some representative ^2H spectra of $^+NH_3$–CH_2–CD_2–DPPE/CHOL mixtures are illustrated in Figure 8. In pure DPPE above T_c a fast-limit powder pattern with a splitting of 9.5 kHz is observed, while below T_c this pattern broadens but its width does not increase dramatically. In addition, there are pronounced decreases in the echo intensity. We have previously interpreted these spectra as indicating that the head group has roughly the same conformation in both the liquid-crystalline and gel phases, but that the motional rates are dramatically different in the two phases (Blume et al., 1982a). We have not attempted to simulate the head group spectra since, as outlined previously, the number of variables

involved is large and a unique fit would probably not be possible (Blume et al., 1982a,b; Skarjune & Oldfield, 1979; Frischleder et al., 1981).

Addition of CHOL to DPPE results in the appearance of the sharp powder pattern at progressively lower temperatures as can be seen in Figure 8. Note that for a given composition, there is good agreement between the ^{13}C and head group spectra as to the temperatures where the sharp component appears. For instance, at 10 and 30 mol % CHOL it is present at 23 and 1 °C, respectively, in both the ^{13}C and ^{2}H spectra. Thus, the conformational change in the glycerol backbone region and fast motion on the ^{2}H time scale in the ethanolamine moiety are clearly related. This observation supports our suggestion that CHOL disrupts the packing that is present in the head group region of pure DPPE bilayers.

In Figure 9a we have plotted $\Delta\nu_{Q\perp}$ of the fast motion component of the spectra, and in Figure 9b the full width at half-height as a function of CHOL concentration for various temperatures. In all cases the splittings or widths of these spectra decrease with increasing CHOL content, although the changes are not large; similar effects have been observed previously in DPPC/CHOL and in DPPE/CHOL mixtures (Brown & Seelig, 1978; Shepherd & Büldt, 1979; Henze, 1980). The plots in Figure 9 show some nonlinear behavior in the two spectral parameters which is different from that observed in, for instance, the acyl chain spectra. The largest changes are observed between 20 and 40% CHOL and indicate some alterations in the average head group conformation. At low temperatures similar behavior is observed.

Previously we mentioned that we have observed some evidence for nonideal mixing of DPPE and CHOL. Specifically, most of the NMR spectra in Figure 8 were recorded starting at temperatures above T_c and decreasing the temperature stepwise to the desired value. Collection of a particular spectrum generally required about 1 h, and we found that samples containing 40 and 50% CHOL exhibited a time-dependent behavior at temperatures below 25 °C. Equilibration of these samples at 10 or 1 °C for 4–5 h to days yielded spectra that were almost identical with those obtained with the 30% CHOL sample. We conclude that rapid cooling of the samples containing more than 30% CHOL to temperatures below 25 °C creates a metastable, nonideal solid solution. Equilibration of these samples at low temperatures then leads to a phase separation of a DPPE/CHOL gel phase with ~30% CHOL content, and possibly a pure CHOL phase, although we have no direct experimental evidence for the latter. Heating these samples to temperatures above 25 °C apparently dissolves the CHOL in the phospholipid bilayer. Since we did not observe a time-dependent behavior above 25 °C, we believe this miscibility gap has a horizontal boundary at about this temperature. Correspondingly no time dependence was observed at CHOL concentrations ≤30%, which indicates a vertical boundary between 30 and 40% CHOL. The same sort of behavior was also seen in the ^{13}C spectra of Figure 1 and the acyl chain spectra of Figure 4. Since the ^{13}C spectra could be collected relatively rapidly, they were quite useful in understanding this phenomenon.

(D) DPPE/CHOL Temperature–Composition Diagram. The ^{13}C and ^{2}H spectra of Figures 1, 4, and 8 can be employed to construct a temperature–composition diagram such as is shown in Figure 10. Included in this figure are data from DSC investigations of this system reported earlier (Blume, 1980). Our purpose in including this diagram is to summarize the changes in the molecular conformation and dynamic properties of DPPE that we derive from our NMR experiments, and to compare these data with those obtained from DSC. This type of plot could obviously be interpreted as a phase diagram. However, for reasons to be discussed below this must be done with caution.

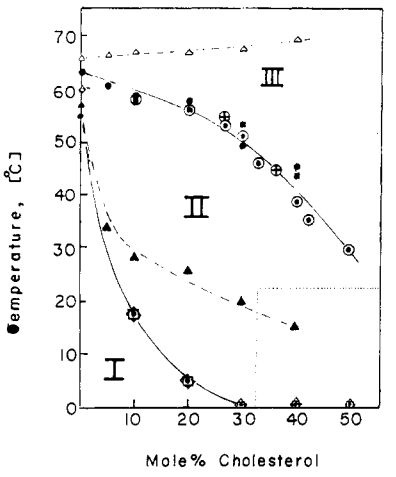

FIGURE 10: Temperature–composition diagram for the DPPE/CHOL system. The dashed lines indicate temperatures for the onset of melting (▲) and completion of melting (△) determined by calorimetry. The solid lines indicate the temperatures and compositions where changes in the NMR spectra are observed. Data points from the NMR experiments that fall on the line separating regions I and II are as follows: (dotted box) first observation of the sharp component in the ^{13}C NMR spectra and (dotted diamond) first appearance of a sharp component in the ^{2}H spectra of $^{+}NH_3$–CH_2–CD_2–DPPE. The position of the line separating regions II and III is determined by (⊙) disappearance of the axially symmetric ^{13}C powder pattern extrapolated from the curves in Figure 2, (⊕) midpoints of the sigmoidal parts of the $\Delta\nu_{Q\perp}$ vs. temperature plots in Figure 5a, and (■) same but obtained from Figure 5b. (●) Midpoints (50% melting) of the integrated heat capacity curves of Figure 2a. The area in the lower right corner of this figure denotes the region where metastable behavior is observed as explained in the text. Uncertainties in the NMR data are estimated to be ±4 °C. For the DSC data they are ±3 °C for $X_{CHOL} \leq 0.2$ and ±5 °C for $X_{CHOL} > 0.2$.

The lowest line in this plot corresponds to the temperatures and compositions where we detect the appearance of a sharp component in the *sn*-2 $^{13}C{=}O$ spectra or the ^{2}H spectra of head group labeled DPPE. For reasons outlined in section B above, we believe the appearance of a sharp component in the acyl chain ^{2}H spectra would also fall on or very near this line. However, since the acyl chain spectra do not always exhibit this sharp component in an obvious way, we have not included these points on this line. The temperatures and compositions in the area to the left of and below this line correspond to a region (labeled I in this figure) where we observe gel-state NMR spectra. The ^{13}C spectra consist of the axially symmetric powder pattern, and the acyl chain spectra and head group spectra are similar to those seen in pure DPPE. The points at 30, 40, and 50 mol % are drawn at 1 °C, although they may extend to slightly lower temperatures. For example, at −15 °C we observe only the axially symmetric powder pattern in the ^{13}C spectra of both the 40 and 50% samples, but the L_α-like line is clearly present and quite intense in the 1 °C spectra of Figure 1.

Immediately above this line we have plotted the temperatures corresponding to the onset of melting observed in the DSC experiments. It is clear that these data correspond in only an approximate fashion to the NMR results, since the two methods monitor somewhat different properties. In particular, the NMR experiments detect microscopic changes in the conformation and dynamic behavior of the particular part of the DPPE molecule that is labeled. In principle DSC can detect any macroscopic change in the thermodynamic

parameters of the system. However, due to finite sensitivity of the calorimeter, only cooperative transitions generally contribute to an endotherm. The broadening of the DSC transition is an obvious indication that the transitions are of lower cooperativity, and this probably explains the differences between the two sets of observations. Nevertheless, the observed differences illustrate that constructing a phase boundary in this temperature–composition region depends on whether one places faith in the NMR or the DSC results. The location of a phase boundary would be different if only one set of experimental data were available.

In the lower right corner of Figure 10 we have drawn a box to indicate the approximate region where we detect metastability in the DPPE/CHOL samples. The observed metastability suggests a vertical phase boundary, perhaps related to a miscibility gap, which can in principle be verified by investigating the long-time behavior of the DPPE/CHOL dispersions with DSC. The exact position of this boundary is at present unknown—e.g., the vertical dashed line could be drawn anywhere between 30 and 40% CHOL. The horizontal boundary probably lies at $T \leq 25$ °C, although again we have not investigated its position carefully.

The next line we have drawn on this diagram delineates the upper boundary of region II and contains data points from three different experiments. First, the curves in Figure 2a derived from the ^{13}C spectra were extrapolated to $f_F = 1$ and provide the temperatures where the axially symmetric ^{13}C powder pattern disappears. Secondly, the splittings in the acyl chain ^2H spectra plotted in Figure 5b exhibit a sigmoidal shape, and the midpoints of these curves are also plotted on this line. In addition, we have included two points that correspond to the well-resolved breaks in the $\Delta\nu_{Q\perp}$ vs. mole percent CHOL curves at 45 and 55 °C shown in Figure 5a. Finally, the midpoints of the integrated heat capacity curves are the third data set that delineate the curve. On a microscopic scale region II of the temperature–composition plot is a region where we detect two long-lived conformations at the *sn*-2 C=O. Viewed with the ^{13}C experiment these two types of molecules appear liquid-crystalline like and gel like in character, and we clearly observe exchange between these two conformations. The data in Figures 2 and 3 indicate that fractional populations are, as expected, temperature and composition dependent. The fact that the simple six-site exchange model can be used to fit the line shapes is evidence that the two types of molecules are in close proximity to one another (100–200 lattice sites). The ^2H spectra of 2[4,4-$^2H_2$]DPPE also show two components, and we have associated the sharp component in these spectra with the fraction that yields the narrow liquid-crystalline-like line in the ^{13}C spectra. At the same time the splittings in the acyl chain spectra are quite large (45–50 kHz). The fluid fraction in region II thus exhibits some, but not all, of the properties of pure L_α-phase DPPE, and should therefore not be thought of as liquid crystalline.

At higher temperatures and CHOL concentrations we enter a region where spectra of liquid-crystalline lipids are observed. The axially symmetric ^{13}C powder pattern is no longer present, the head group spectra are sharp, and the acyl chains have disordered and exhibit splittings of ≤40 kHz. For comparison we have also included in this region points corresponding to the temperatures for completion of melting obtained from the DSC experiments. As is obvious from the plot, they do not coincide to the NMR data, and thus again there is some latitude in the choice of where a phase boundary would be constructed. In addition, at high CHOL concentration—e.g., 50 mol %—the acyl chain splittings do not show a clear break as a function of temperature. Because of this, it becomes more difficult to differentiate between the fluid fraction observed at lower CHOL contents and the liquid-like phases seen in region III.

Conclusions. The thermal behavior of pure DPPE bilayers is somewhat simpler than diacyl-PC's in that they exhibit a single L_β gel phase below the main transition temperature. Correspondingly, the DPPE/CHOL system appears to behave in a relatively simple fashion, and the results of our ^{13}C and ^2H NMR experiments can be easily interpreted. NMR spectra of *sn*-2 ^{13}C=O labeled DPPE show a characteristic change in the line shape from an axially symmetric powder pattern in the L_β phase to an isotropic-like line in the L_α phase. This spectral alteration is due to a conformational change in the glycerol backbone region that occurs as the bilayer expands. Addition of CHOL to DPPE also induces this conformational change, and it occurs at progressively lower temperatures with increasing CHOL concentration. As a consequence, a sharp component is visible in the ^{13}C spectra well below the onset of melting determined by DSC. Concurrently, ^2H spectra of acyl chain and head group labeled DPPE indicate the presence of a fraction of molecules undergoing fast axial diffusion. Apparently, CHOL can be viewed as a spacer that disrupts the packing present in pure DPPE bilayers, and this leads to the observed spectral changes. At many temperatures and compositions, two components are visible in the spectra, which is convincing evidence for the presence of two conformationally and dynamically inequivalent molecules. The spectral parameters indicate that one of these can be classified as a gel-state DPPE molecule with reasonable accuracy. However, the second has conformational and dynamic properties of both gel- and liquid-crystalline-phase lipids. Specifically, the conformation in the backbone region is similar to that seen in the L_α phase, and it diffuses rapidly on the ^2H time scale about its long axis, which is also characteristic of L_α-phase lipids. However, with increasing temperature the acyl chains undergo a cooperative transition to a higher degree of disorder. The fact that this transition is observed clearly distinguishes these fluid "liquid gelatin" lipids from those seen in the conventional liquid-crystalline phase.

The interpretation of the NMR data in terms of a thermodynamic phase diagram must be done with caution. As we have seen above certain changes in the NMR spectra can be related to, for example, DSC results, but in other cases this is not possible. The reason for these differences is apparently related to the fact that phase transitions in these systems are not in general highly cooperative. On a microscopic scale it appears that "domains" in the DPPE/CHOL system are small, and as a result a DPPE molecule can sample CHOL-rich and -poor regions in a short time period. The same is not true in, for instance, the DPPC/DPPE system. In this case the domains are large, the transitions observed in the DSC experiment are sharper, and they coincide directly to changes in the NMR spectra. Thus, there may or may not exist a simple relation between the macroscopic thermodynamic behavior and the NMR spectra. Nevertheless, the ^{13}C and ^2H NMR results described here indicate that a wealth of information on molecular conformation and dynamics is available from the spectra, and investigations of other lipid/CHOL mixtures with these techniques may be equally fruitful. Because of its relative simplicity, the DPPE/CHOL system should serve as a basis for the interpretation of such experiments.

Acknowledgments

We thank our colleagues R. J. Wittebort, D. M. Rice, T-H. Huang, S. K. Das Gupta, and D. J. Ruben for their assistance

in various parts of this work and for their stimulating conversations.

References

Bienvenue, A., Bloom, M., Davis, J. H., & Devaux, P. F. (1982) *J. Biol. Chem. 257*, 3032.

Blume, A. (1980) *Biochemistry 19*, 4908.

Blume, A., Rice, D., Wittebort, R. J., & Griffin, R. G. (1982a) *Biochemistry* (first paper of three in this issue).

Blume, A., Wittebort, R. J., Das Gupta, S. K., & Griffin, R. G. (1982b) *Biochemistry* (third paper of three in this issue).

Brown, M. F., & Seelig, J. (1978) *Biochemistry 17*, 381.

Calhoun, W. I., & Shipley, G. G. (1979) *Biochemistry 18*, 1717.

Copeland, B. R., & McConnell, H. M. (1980) *Biochim. Biophys. Acta 599*, 95.

Cornell, B. A., Chapman, D., & Peel, W. E. (1979) *Chem. Phys. Lipids 23*, 223.

Davis, J. H., Jeffrey, K. R., Bloom, M., Valic, M. I., & Higgs, T. P. (1976) *Chem. Phys. Lett. 42*, 390.

Demel, R. A., & deKruijff (1976) *Biochim. Biophys. Acta 457*, 109.

Estep, T. N., Mountcastle, D. B., Biltonen, R. L., & Thompson, T. E. (1978) *Biochemistry 17*, 1984.

Estep, T. N., Mountcastle, D. B., Barenholz, Y., Biltonen, R. L., & Thompson, T. E. (1979) *Biochemistry 18*, 2112.

Frischleder, H., Krahl, R., & Lehmann, E. (1981) *Chem. Phys. Lipids 28*, 291.

Gershfeld, N. L. (1978) *Biophys. J. 22*, 469.

Griffin, R. G. (1981) *Methods Enzymol. 72*, 108.

Haberkorn, R. A., Griffin, R. G., Meadows, M. D., & Oldfield, E. (1977) *J. Am. Chem. Soc. 99*, 7353.

Henze, R. (1980) *Chem. Phys. Lipids 27*, 165.

Hui, S. W. (1981) *Biophys. J. 34*, 383.

Jacobs, R., & Oldfield, E. (1979) *Biochemistry 18*, 3280.

Kang, S. Y., Gutowsky, H. S., Huang, J. C., Jacobs, R., King, T. E., Rice, D. M., & Oldfield, E. (1979) *Biochemistry 18*, 3257.

Ladbrooke, B. D., Williams, R. M., & Chapman, D. (1968) *Biochim. Biophys. Acta 150*, 333.

Lentz, B. R., Barrow, D. A., & Hoechli, M. (1980) *Biochemistry 19*, 1943.

Mabrey, S., Mateo, P. L., & Sturtevant, J. M. (1978) *Biochemistry 17*, 2646.

Maraviglia, B., Davis, J. H., Bloom, M., Westerman, J., & Wertz, K. W. A. (1982) *Biochim. Biophys. Acta* (in press).

Melchior, D. L., Scavitto, F. J., & Steim, J. M. (1980) *Biochemistry 19*, 4828.

Müller-Landau, F., & Cadenhead, D. A. (1979) *Chem. Phys. Lipids 25*, 315.

Owicki, J. C., & McConnell, H. M. (1980) *Biophys. J. 30*, 383.

Paddy, M. R., Dahlquist, F. W., Davis, J. H., & Bloom, M. (1981) *Biochemistry 20*, 3152.

Phillips, M. C. (1972) *Prog. Surf. Membr. Sci. 5*, 139.

Pines, A., Gibby, M. G., & Waugh, J. S. (1973) *J. Chem. Phys. 59*, 569.

Pink, D., & Chapman, D. (1979) *Proc. Natl. Acad. Sci. U.S.A. 76*, 1542.

Recktenwald, D. J., & McConnell, H. M. (1981) *Biochemistry 20*, 4505.

Rice, D. M., Hsung, J. C., King, T. E., & Oldfield, E. (1979) *Biochemistry 18*, 5885.

Rubinstein, J. L. R., Smith, B. A., & McConnell, H. M. (1979) *Proc. Natl. Acad. Sci. U.S.A. 76*, 15.

Rubinstein, J. L. R., Owicki, J. C., & McConnell, H. M. (1980) *Biochemistry 19*, 569.

Seelig, J., Tamm, L., Hymel, L., & Fleischer, S. (1981) *Biochemistry 20*, 3922.

Shah, D. O., & Schulman, D. H. (1967) *J. Lipid Res. 8*, 215.

Shepherd, J. C. W., & Büldt, G. (1979) *Biochim. Biophys. Acta 558*, 41.

Shimshick, E. J., & McConnell, H. M. (1973) *Biochem. Biophys. Res. Commun. 53*, 446.

Skarjune, R., & Oldfield, E. (1979) *Biochemistry 18*, 5903.

Snyder, B., & Freire, E. (1980) *Proc. Natl. Acad. Sci. U.S.A. 77*, 4055.

Spiess, H. W., & Sillescu, H. (1981) *J. Magn. Reson. 42*, 381.

Wittebort, R. G., Schmidt, C. F., & Griffin, R. G. (1981) *Biochemistry 20*, 4223.

Wittebort, R. G., Blume, A., Huang, T-H., Das Gupta, S. K., & Griffin, R. G. (1982) *Biochemistry 21*, 3487.